Lattice regularization for chiral perturbation theory

Randy Lewis and Pierre-Philippe A. Ouimet

Department of Physics, University of Regina, Regina, SK, Canada S4S 0A2

(October 2000)

The SU(3) chiral Lagrangian for the lightest octets of mesons and baryons is constructed on a spacetime lattice. The lattice spacing acts as an ultraviolet momentum cutoff which appears directly in the Lagrangian so chiral symmetry remains explicit. As the lattice spacing vanishes, Feynman loop diagrams typically become divergent due to inverse powers of the lattice spacing, and these divergences get absorbed into counterterms such that the standard results of dimensional regularization are obtained. One advantage of lattice regularization is that power divergences are seen explicitly. In the present work, the octet meson masses, the octet baryon masses and the πN sigma term are all computed explicitly to one loop order.

I. INTRODUCTION

Chiral perturbation theory (ChPT) [1] is a low momentum effective field theory for QCD. For the physics of pions, kaons and eta mesons, ChPT organizes the infinite set of possible interactions into a systematic expansion in inverse powers of the chiral scale, Λ_χ. Although no precise definition of Λ_χ is required, it is understood to be O(1 GeV):

$$\Lambda_\chi \sim m_\rho \sim 4\pi F_\pi \sim 4\pi F_K \sim 1 \text{ GeV}. \tag{1}$$

Powers of $4\pi F$ appear as natural suppression factors in the calculation of the loop diagrams in ChPT, and the ρ meson is the lightest hadron which does not appear explicitly in the ChPT Lagrangian. The crucial test of ChPT comes from the explicit calculation of observables to see whether higher order terms in the expansion really give smaller contributions, and the literature contains many such successful examples. [2]

Since no baryon is light in comparison to Λ_χ, it is difficult to include them into ChPT without destroying the systematic expansion. Recent work on baryon ChPT is producing interesting new suggestions [3], but we will use the traditional solution, heavy baryon ChPT (HBChPT) [4], which is a double expansion in $1/\Lambda_\chi$ and $1/m_{\text{baryon}}$.

In the present work, the chiral Lagrangian is constructed on a spacetime lattice, where the inverse lattice spacing plays the role of a momentum cutoff. Because the lattice spacing appears directly in the chirally-symmetric Lagrangian, the chiral properties of calculations are assured. The lattice-regularized HBChPT Lagrangian is not unique (we will choose an isotropic hypercubic lattice) but the continuum limit is unique and is the familiar continuum-defined chiral Lagrangian. Since observable quantities cannot depend on the regularization and renormalization prescriptions, any valid lattice implementation must reproduce the results of dimensional regularization in the limit of vanishing lattice spacing.

In contrast to dimensional regularization, lattice regularization shows the power divergences explicitly. These divergences can also be seen with a nonlattice cutoff, but this is typically invoked at the time of integration rather than directly in the Lagrangian, so care is required to be sure that chiral symmetry is not violated by the cutoff procedure. One example of research that relies upon information about power divergences is found in Ref. [5], where a nonlattice cutoff was used to discuss the convergence of HBChPT and the scale of baryon substructure.

Lattice QCD simulations are always performed with a nonzero lattice spacing, and they typically use unphysical quark masses as well. ChPT is regularly employed for the extrapolations to physical results. [6] Lattice-regularized ChPT offers an analytic way to study discretization errors in these chiral extrapolations. Although lattice-regularized ChPT does not have a unique Lagrangian, it does allow a determination of the typical size of discretization errors as a function of the quark masses and the lattice spacing. The connection between lattice ChPT and lattice QCD has been discussed in Ref. [7] in the limits of strong coupling and large N_c.

In section II of the present work, an SU(3) meson Lagrangian is constructed at leading and next-to-leading chiral order on a spacetime lattice, and the meson masses and renormalization constants are calculated. This allows a comparison to the work of Shushpanov and Smilga [8] who calculated the quadratically-divergent pieces of F_π, m_π and wavefunction renormalization in an SU(2) lattice theory. Section III of the present work contains

the meson-baryon Lagrangian. A calculation of the baryon masses and the pion-nucleon sigma term is shown to produce the familiar dimensional regularization results as the lattice spacing approaches zero. In section IV, the baryon masses and the pion-nucleon sigma term are discussed for nonzero lattice spacing, and section V contains a concluding discussion.

II. THE MESON LAGRANGIAN

When the standard SU(3) ChPT Lagrangian of Gasser and Leutwyler [9] is written in Euclidean spacetime, it takes the following form,

$$\mathcal{L}_{\mathrm{M}} = \mathcal{L}_{\mathrm{M}}^{(2)} + \mathcal{L}_{\mathrm{M}}^{(4)}, \tag{2}$$

$$\mathcal{L}_{\mathrm{M}}^{(2)} = \frac{F^2}{4} \mathrm{Tr}\{\sum_{\mu} \nabla_\mu U^\dagger \nabla_\mu U - \chi^\dagger U - \chi U^\dagger\}, \tag{3}$$

$$\begin{aligned}
\mathcal{L}_{\mathrm{M}}^{(4)} = &-L_1 \left(\sum_\mu \mathrm{Tr}\{\nabla_\mu U^\dagger \nabla_\mu U\} \right)^2 - L_2 \sum_{\mu,\nu} \mathrm{Tr}\{\nabla_\mu U^\dagger \nabla_\nu U\} \mathrm{Tr}\{\nabla_\mu U^\dagger \nabla_\nu U\} \\
&-L_3 \sum_{\mu,\nu} \mathrm{Tr}\{\nabla_\mu U^\dagger \nabla_\mu U \nabla_\nu U^\dagger \nabla_\nu U\} + L_4 \sum_\mu \mathrm{Tr}\{\nabla_\mu U^\dagger \nabla_\mu U\} \mathrm{Tr}\{\chi^\dagger U + \chi U^\dagger\} \\
&+L_5 \sum_\mu \mathrm{Tr}\{\nabla_\mu U^\dagger \nabla_\mu U(\chi^\dagger U + U^\dagger \chi)\} - L_6 \left(\mathrm{Tr}\{\chi^\dagger U + \chi U^\dagger\} \right)^2 \\
&-L_7 \left(\mathrm{Tr}\{\chi^\dagger U - \chi U^\dagger\} \right)^2 - L_8 \mathrm{Tr}\{\chi^\dagger U \chi^\dagger U + \chi U^\dagger \chi U^\dagger\} \\
&+iL_9 \sum_{\mu,\nu} \mathrm{Tr}\{F_{\mu\nu}^R \nabla_\mu U \nabla_\nu U^\dagger + F_{\mu\nu}^L \nabla_\mu U^\dagger \nabla_\nu U\} - L_{10} \sum_{\mu,\nu} \mathrm{Tr}\{U^\dagger F_{\mu\nu}^R U F_{\mu\nu}^L\}, \tag{4}
\end{aligned}$$

where $U(x)$ is a nonlinear representation of the pseudoscalar meson octet, and the current quark mass matrix, $\mathcal{M}$, enters via

$$\chi = 2B\mathcal{M}. \tag{5}$$

External vector and axial vector fields appear within the covariant derivative, $\nabla_\mu U(x)$, and within the field strengths, $F_{\mu\nu}^L(x)$ and $F_{\mu\nu}^R(x)$.

The chiral transformation of $U(x)$ is

$$U(x) \rightarrow g(x)U(x)h(x), \tag{6}$$

where $g(x) \in SU_R(3)$ and $h(x) \in SU_L(3)$. On a spacetime lattice, we introduce the parallel transporters, $R_\mu(x) \in SU_R(3)$ and $L_\mu(x) \in SU_L(3)$, which transform as

$$R_\mu(x) \rightarrow g(x)R_\mu(x)g^\dagger(x + a_\mu), \tag{7}$$

$$L_\mu(x) \rightarrow h^\dagger(x)L_\mu(x)h(x + a_\mu). \tag{8}$$

a_μ is a Euclidean vector of length a in the μ direction, and a is the lattice spacing. The Lie algebra-valued vector and axial vector fields, $V_\mu(x)$ and $A_\mu(x)$, appear in the exponents,

$$L_\mu(x) = \exp\{-ia\ell_\mu(x)\}, \tag{9}$$

$$R_\mu(x) = \exp\{-iar_\mu(x)\}, \tag{10}$$

3

where $\ell_\mu(x) = V_\mu(x) - A_\mu(x)$ and $r_\mu(x) = V_\mu(x) + A_\mu(x)$. In $\mathcal{L}_{\mathrm{M}}^{(2)}$, the following covariant derivative is used,

$$\nabla_\mu^{(+)} U(x) = \frac{1}{a} \left\{ R_\mu(x) U(x + a_\mu) L_\mu^\dagger(x) - U(x) \right\}, \tag{11}$$

but for all other Lagrangian terms (in $\mathcal{L}_{\mathrm{M}}^{(4)}$, $\mathcal{L}_{\mathrm{M}}^{(6)}$, ...) a more symmetric derivative is used:

$$\nabla_\mu^{(\pm)} U(x) = \frac{1}{2a} \left\{ R_\mu(x) U(x + a_\mu) L_\mu^\dagger(x) - R_\mu^\dagger(x - a_\mu) U(x - a_\mu) L_\mu(x - a_\mu) \right\}. \tag{12}$$

Use of $\nabla_\mu^{(\pm)}$ at leading order would produce extraneous poles in the meson propagator ("doublers") and use of $\nabla_\mu^{(+)}$ in higher order Lagrangian terms can violate parity.

The lattice ChPT action is simply obtained by summing the Lagrangian over all spacetime lattice sites,

$$S_{\mathrm{M}}[U, V_\mu, A_\mu] = a^4 \sum_x \mathcal{L}_{\mathrm{M}}(x). \tag{13}$$

The propagators and vertices required for perturbative calculations can be extracted from this action, but if the path integral formalism is used, one must pay particular attention to extra meson interactions which get generated by the integration measure,

$$DU = e^{-S_{\mathrm{meas}}[\pi]} \prod_{a=1}^{8} \mathrm{d}\pi^a, \tag{14}$$

The definition $U(x) = \exp\{-i\lambda^a \pi^a(x)/F\}$ has been employed; λ^a is a Gell-Mann matrix and $\pi^a(x)$ is a pseudoscalar meson field. The "effective action" from the measure is [10]

$$S_{\mathrm{meas}}[\pi] = -\frac{1}{2} \sum_x \mathrm{Tr} \ln \left\{ \frac{2(1 - \cos \Phi(x))}{\Phi^2(x)} \right\}, \tag{15}$$

$$\Phi(x) = \frac{2}{F} \sum_{a=1}^{8} t^a \pi^a(x), \tag{16}$$

where $t_{bc}^a = -i f_{abc}$ and f_{abc} are the structure constants defined by $[\lambda^a, \lambda^b] = 2i f^{abc} \lambda^c$. These measure contributions also exist in the continuum theory, although they happen to vanish when dimensional regularization is used.

Neglecting isospin violation and using m_l to denote the up and down quark masses, the lowest order pion, kaon and eta two point functions are

$$\Gamma_{MM} = - \left\{ x_M^2 + \frac{4}{a^2} \sum_\mu \sin^2 \left(\frac{a q_\mu}{2} \right) \right\}, \tag{17}$$

where

$$x_\pi = \sqrt{2 B m_l}, \tag{18}$$

$$x_K = \sqrt{B(m_l + m_s)}, \tag{19}$$

$$x_\eta = \sqrt{\frac{2}{3} B(m_l + 2 m_s)}. \tag{20}$$

4

The meson masses are obtained from the zero of Eq. (17), corresponding to the pole in the propagator,

$$m_M = \frac{2}{a}\text{arcsinh}\left(\frac{ax_M}{2}\right). \tag{21}$$

Notice the existence of a Gell-Mann–Okubo relation,

$$3\sinh^2\left(\frac{am_\eta}{2}\right) = 4\sinh^2\left(\frac{am_K}{2}\right) - \sinh^2\left(\frac{am_\pi}{2}\right), \tag{22}$$

which reproduces the conventional relation as $a \to 0$.

At next-to-leading order, the meson masses receive tree-level contributions from $\mathcal{L}_M^{(4)}$ and from $S_{\text{meas}}[\pi]$ as well as loop diagrams from the interactions of $\mathcal{L}_M^{(2)}$. The only loop topology at this order is shown in Fig. 1 and, for example, a charged kaon loop makes the following addition to the pion two-point function,

$$\Delta\Gamma_{\pi\pi} = \frac{1}{3a^2F^2}\int_{-\pi/a}^{\pi/a}\frac{\mathrm{d}^4p}{(2\pi)^4}\left\{x_K^2 + \frac{4}{a^2}\sum_\nu\sin^2\left(\frac{ap_\nu}{2}\right)\right\}^{-1}$$
$$\times\left(\frac{a^2}{2}(x_\pi^2 + x_K^2) + \sum_\mu\{5 - 4\cos(aq_\mu) - 4\cos(ap_\mu) + 3\cos(aq_\mu - ap_\mu)\}\right). \tag{23}$$

Notice that only momenta within the first Brillouin zone can appear in the integral, since physics at shorter distances cannot be resolved on the spacetime lattice. The integral is thus finite, and only diverges as $a \to 0$. It is convenient to rewrite the propagator within Eq. (23) as the integral of an exponential, using $1/D = \int_0^\infty \mathrm{d}x\,\exp(-xD)$, which leads to

$$\Delta\Gamma_{\pi\pi} = \frac{1}{6a^4F^2}\left\{1 + \frac{a^2x_\pi^2}{2}W_4(a^2x_K^2)\right\}$$
$$+ \frac{1}{4a^4F^2}\left\{1 + \frac{4}{3}\left(1 - \frac{3}{8}a^2x_K^2\right)W_4(a^2x_K^2)\right\}\sum_\mu\sin^2\left(\frac{aq_\mu}{2}\right), \tag{24}$$

where

$$W_n(\epsilon^2) \equiv \int_0^\infty \mathrm{d}x\,I_0^n(x)\exp\left\{-x\left(n + \frac{\epsilon^2}{2}\right)\right\} \tag{25}$$

and $I_0(x)$ is a Bessel function,

$$I_0(x) = \int_{-\pi}^\pi \frac{\mathrm{d}\theta}{2\pi}\,\exp(x\cos\theta). \tag{26}$$

By including all of the one-loop diagrams and $\mathcal{L}_M^{(4)}$ tree-level pieces, the complete two point functions to next-to-leading order are found to be

$$\Gamma_{MM} = -\frac{1}{Z_M^{(+)}Z_M^{(\pm)}}\left\{X_M^2 + \frac{4Z_M^{(\pm)}}{a^2}\sum_\mu\sin^2\left(\frac{aq_\mu}{2}\right) + \left(\frac{1 - Z_M^{(\pm)}}{a^2}\right)\sum_\mu\sin^2(aq_\mu)\right\} \tag{27}$$

5

with

$$Z_\pi^{(+)} = 1 + \frac{7}{24a^2F^2} + \frac{1}{3a^2F^2}\left(1 - \frac{3}{16}a^2x_\pi^2\right)W_4(a^2x_\pi^2)$$
$$+ \frac{1}{6a^2F^2}\left(1 - \frac{3}{8}a^2x_K^2\right)W_4(a^2x_K^2) - \frac{x_\eta^2}{48F^2}W_4(a^2x_\eta^2), \tag{28}$$

$$Z_\pi^{(\pm)} = 1 - \frac{8}{F^2}(x_\pi^2 + 2x_K^2)L_4 - \frac{8}{F^2}x_\pi^2 L_5, \tag{29}$$

$$Z_K^{(+)} = 1 + \frac{7}{24a^2F^2} + \frac{1}{8a^2F^2}\left(1 - \frac{3}{8}a^2x_\pi^2\right)W_4(a^2x_\pi^2)$$
$$+ \frac{1}{4a^2F^2}\left(1 - \frac{3}{8}a^2x_K^2\right)W_4(a^2x_K^2) + \frac{1}{8a^2F^2}\left(1 - \frac{1}{24}a^2x_\eta^2\right)W_4(a^2x_\eta^2), \tag{30}$$

$$Z_K^{(\pm)} = 1 - \frac{8}{F^2}(x_\pi^2 + 2x_K^2)L_4 - \frac{8}{F^2}x_K^2 L_5, \tag{31}$$

$$Z_\eta^{(+)} = 1 + \frac{7}{24a^2F^2} - \frac{x_\pi^2}{16F^2}W_4(a^2x_\pi^2)$$
$$+ \frac{1}{2a^2F^2}\left(1 - \frac{1}{24}a^2x_K^2\right)W_4(a^2x_K^2) - \frac{x_\eta^2}{16F^2}W_4(a^2x_\eta^2), \tag{32}$$

$$Z_\eta^{(\pm)} = 1 - \frac{8}{F^2}(x_\pi^2 + 2x_K^2)L_4 - \frac{8}{F^2}x_\eta^2 L_5, \tag{33}$$

$$X_\pi^2 = x_\pi^2 - \frac{8}{F^2}x_\pi^2(x_\pi^2 + 2x_K^2)(L_4 - 2L_6) - \frac{8}{F^2}x_\pi^4(L_5 - 2L_8)$$
$$+ \frac{7x_\pi^2}{24a^2F^2} + \frac{x_\pi^2}{4a^2F^2}\left\{W_4(a^2x_\pi^2) - \frac{1}{3}W_4(a^2x_\eta^2)\right\}$$
$$- \frac{x_\pi^4}{16F^2}W_4(a^2x_\pi^2) - \frac{x_\pi^2x_K^2}{16F^2}W_4(a^2x_K^2) - \frac{x_\pi^2x_\eta^2}{48F^2}W_4(a^2x_\eta^2), \tag{34}$$

$$X_K^2 = x_K^2 - \frac{8}{F^2}x_K^2(x_\pi^2 + 2x_K^2)(L_4 - 2L_6) - \frac{8}{F^2}x_K^4(L_5 - 2L_8)$$
$$+ \frac{7x_K^2}{24a^2F^2} + \frac{x_K^2}{6a^2F^2}W_4(a^2x_\eta^2)$$
$$- \frac{3x_\pi^2x_K^2}{64F^2}W_4(a^2x_\pi^2) - \frac{3x_K^4}{32F^2}W_4(a^2x_K^2) - \frac{x_K^2x_\eta^2}{192F^2}W_4(a^2x_\eta^2), \tag{35}$$

$$X_\eta^2 = x_\eta^2 - \frac{8}{F^2}x_\eta^2(x_\pi^2 + 2x_K^2)(L_4 - 2L_6) - \frac{8}{F^2}x_\eta^4(L_5 - 2L_8) + \frac{128}{9F^2}(x_K^2 - x_\pi^2)^2(3L_7 + L_8)$$
$$+ \frac{7x_\eta^2}{24a^2F^2} - \frac{x_\pi^2}{4a^2F^2}W_4(a^2x_\pi^2) + \frac{(x_\pi^2 + 3x_\eta^2)}{6a^2F^2}W_4(a^2x_K^2) + \frac{(7x_\pi^2 - 16x_K^2)}{36a^2F^2}W_4(a^2x_\eta^2)$$
$$- \frac{x_\pi^2x_\eta^2}{16F^2}W_4(a^2x_\pi^2) - \frac{x_K^2x_\eta^2}{48F^2}W_4(a^2x_K^2) - \frac{x_\eta^4}{16F^2}W_4(a^2x_\eta^2). \tag{36}$$

The physical meson masses are obtained by using X_M instead of x_M in Eq. (21). Notice that the pseudoscalar mesons are exactly massless in the chiral limit ($m_l = m_s = 0$), indicating that the theory does indeed have exact chiral symmetry even for nonzero lattice spacing. This feature has been emphasized in the SU(2) case by the authors of Ref. [8].

The lattice regularized theory gives finite predictions for all observables at nonzero lattice spacing. The chiral expansion is in inverse powers of Λ_χ. If one chooses to extrapolate to

6

the limit of vanishing lattice spacing, then divergences appear in the loop contributions and they must be absorbed into renormalized values of the Lagrangian parameters. With the information in Appendix A, it is a simple matter to show that the continuum limit of the lattice theory gives precisely the masses that are familiar from dimensional regularization. [9] Moreover, the logarithmic dependences of the counterterms are found to be

$$L_4^r(1/a_2) - 2L_6^r(1/a_2) - \{L_4^r(1/a_1) - 2L_6^r(1/a_1)\} = -\frac{1}{36(4\pi)^2} \ln\left(\frac{a_2}{a_1}\right), \tag{37}$$

$$L_5^r(1/a_2) - 2L_8^r(1/a_2) - \{L_5^r(1/a_1) - 2L_8^r(1/a_1)\} = \frac{1}{6(4\pi)^2} \ln\left(\frac{a_2}{a_1}\right), \tag{38}$$

$$3L_7^r(1/a_2) + L_8^r(1/a_2) - \{3L_7^r(1/a_1) + L_8^r(1/a_1)\} = \frac{5}{48(4\pi)^2} \ln\left(\frac{a_2}{a_1}\right), \tag{39}$$

for sufficiently small lattice spacings a_1 and a_2. This is precisely the scale dependence that is known from Ref. [9], as required, since observables cannot depend on the regularization prescription.

III. THE MESON-BARYON LAGRANGIAN

The HBChPT Lagrangian is organized as a systematic expansion in the inverse baryon mass as well as the inverse chiral scale, Λ_χ. This is accomplished by writing the Lagrangian in terms of a heavy baryon field, $B_v(x)$, instead of the relativistic field, $B(x)$, as follows,

$$B_v(x) = \exp(im_{\mathrm{HB}} v \cdot x)\frac{1}{2}(1 + \slashed{v})B(x), \tag{40}$$

where the mass parameter m_{HB} is chosen to cancel, or nearly cancel, the octet baryon masses. The first few orders in the double expansion of HBChPT are well known [4], and in Euclidean spacetime one finds

$$\mathcal{L}_{\mathrm{MB}} = \mathcal{L}_{\mathrm{MB}}^{(0)} + \mathcal{L}_{\mathrm{MB}}^{(1)} + \mathcal{L}_{\mathrm{MB}}^{(2)} + \mathcal{L}_{\mathrm{MB}}^{(3)} + \text{ higher order}, \tag{41}$$

$$\mathcal{L}_{\mathrm{MB}}^{(0)} = (m_0 - m_{\mathrm{HB}})\mathrm{Tr}\left(\bar{B}_v B_v\right), \tag{42}$$

$$\mathcal{L}_{\mathrm{MB}}^{(1)} = \sum_\mu \left[\mathrm{Tr}\left(\bar{B}_v v_\mu D_\mu B_v\right) + \mathcal{D}\mathrm{Tr}\left(\bar{B}_v S_\mu \{u_\mu, B_v\}\right) + \mathcal{F}\mathrm{Tr}\left(\bar{B}_v S_\mu [u_\mu, B_v]\right)\right], \tag{43}$$

$$\mathcal{L}_{\mathrm{MB}}^{(2)} = \frac{1}{2m_0}\mathrm{Tr}\left(\bar{B}_v(v \cdot D v \cdot D - D^2)B_v\right) - b_{\mathcal{D}}\mathrm{Tr}\left(\bar{B}_v\{\chi_+, B_v\}\right) - b_{\mathcal{F}}\mathrm{Tr}\left(\bar{B}_v[\chi_+, B_v]\right)$$
$$- b_0 \mathrm{Tr}\left(\bar{B}_v B_v\right)\mathrm{Tr}\left(\chi_+\right) + \ldots, \tag{44}$$

$$\mathcal{L}_{\mathrm{MB}}^{(3)} = \ldots, \tag{45}$$

where the omitted terms do not contribute to the present work. m_0 is the leading contribution to the octet baryon mass that would appear in a relativistic Lagrangian, $\mathcal{D}$ and $\mathcal{F}$ are the two axial couplings, and $S_\mu = \frac{i}{2}\gamma_5 \sum_\nu \sigma_{\mu\nu} v_\nu$ is the Pauli-Lubanski spin vector. The matrix B_v denotes the baryon octet,

$$B_v = \begin{pmatrix} \frac{1}{\sqrt{2}}\Sigma_v^0 + \frac{1}{\sqrt{6}}\Lambda_v & \Sigma_v^+ & p_v \\ \Sigma_v^- & -\frac{1}{\sqrt{2}}\Sigma_v^0 + \frac{1}{\sqrt{6}}\Lambda_v & n_v \\ \Xi_v^- & \Xi_v^0 & -\frac{2}{\sqrt{6}}\Lambda_v \end{pmatrix}, \tag{46}$$

while the pseudoscalar mesons appear within $U = \xi^2$ and $\chi_+ = \xi^\dagger \chi \xi^\dagger + \xi \chi^\dagger \xi$. The hadron fields transform under local chiral transformations as

$$B_v(x) \rightarrow o(x)B_v(x)o^\dagger(x), \tag{47}$$
$$\xi(x) \rightarrow g(x)\xi(x)o^\dagger(x) = o(x)\xi(x)h(x). \tag{48}$$

It is convenient to choose $v = (0,0,0,1)$, and to use a nearest-neighbour covariant derivative in the time direction,

$$
\begin{aligned}
aD_4 B_v(x) = \;& B_v(x) \\
& - \frac{1}{4}\xi^\dagger(x)R_4^\dagger(x-a_4)\xi(x-a_4)B_v(x-a_4)\xi^\dagger(x-a_4)R_4(x-a_4)\xi(x) \\
& - \frac{1}{4}\xi(x)L_4^\dagger(x-a_4)\xi^\dagger(x-a_4)B_v(x-a_4)\xi(x-a_4)L_4(x-a_4)\xi^\dagger(x) \\
& - \frac{1}{4}\xi^\dagger(x)R_4^\dagger(x-a_4)\xi(x-a_4)B_v(x-a_4)\xi(x-a_4)L_4(x-a_4)\xi^\dagger(x) \\
& - \frac{1}{4}\xi(x)L_4^\dagger(x-a_4)\xi^\dagger(x-a_4)B_v(x-a_4)\xi^\dagger(x-a_4)R_4(x-a_4)\xi(x).
\end{aligned} \tag{49}
$$

Spatial covariant derivatives appear in $\mathcal{L}_{\mathrm{MB}}^{(2)} + \mathcal{L}_{\mathrm{MB}}^{(3)} + \ldots$, and for these a symmetric definition is used (to conserve parity):

$$
\begin{aligned}
aD_j B_v(x) = \;& \frac{1}{8}\xi(x)L_j(x)\xi^\dagger(x+a_j)B_v(x+a_j)\xi(x+a_j)L_j^\dagger(x)\xi^\dagger(x) \\
& + \frac{1}{8}\xi^\dagger(x)R_j(x)\xi(x+a_j)B_v(x+a_j)\xi(x+a_j)L_j^\dagger(x)\xi^\dagger(x) \\
& + \frac{1}{8}\xi(x)L_j(x)\xi^\dagger(x+a_j)B_v(x+a_j)\xi^\dagger(x+a_j)R_j^\dagger(x)\xi(x) \\
& + \frac{1}{8}\xi^\dagger(x)R_j(x)\xi(x+a_j)B_v(x+a_j)\xi^\dagger(x+a_j)R_j^\dagger(x)\xi(x) \\
& - \frac{1}{8}\xi^\dagger(x)R_j^\dagger(x-a_j)\xi(x-a_j)B_v(x-a_j)\xi^\dagger(x-a_j)R_j(x-a_j)\xi(x) \\
& - \frac{1}{8}\xi(x)L_j^\dagger(x-a_j)\xi^\dagger(x-a_j)B_v(x-a_j)\xi(x-a_j)L_j(x-a_j)\xi^\dagger(x) \\
& - \frac{1}{8}\xi^\dagger(x)R_j^\dagger(x-a_j)\xi(x-a_j)B_v(x-a_j)\xi(x-a_j)L_j(x-a_j)\xi^\dagger(x) \\
& - \frac{1}{8}\xi(x)L_j^\dagger(x-a_j)\xi^\dagger(x-a_j)B_v(x-a_j)\xi^\dagger(x-a_j)R_j(x-a_j)\xi(x).
\end{aligned} \tag{50}
$$

One also defines

$$u_\mu(x) = \frac{i}{2}\xi^\dagger(x)\nabla_\mu^{(\pm)}U(x)\xi^\dagger(x) - \frac{i}{2}\xi(x)\nabla_\mu^{(\pm)}U^\dagger(x)\xi(x), \tag{51}$$

8

where $\nabla_\mu^{(\pm)}U(x)$ is given by Eq. (12).

From $\mathcal{L}_{\rm MB}^{(0)} + \mathcal{L}_{\rm MB}^{(1)}$, the lowest order baryon two-point function is

$$\Gamma_{BB} = m_{\rm HB} - m_0 - \frac{i}{a}\left\{\sin(aq_4) - 2i\sin^2\left(\frac{aq_4}{2}\right)\right\}, \tag{52}$$

which has a unique zero in the first Brillouin zone, occurring at

$$E \equiv -ip_4 = \frac{1}{a}\ln\{1 + a(m_0 - m_{\rm HB})\}. \tag{53}$$

The physical baryon mass is then $m_{\rm HB} + E = m_0 + O(a)$. Typically the parameter $m_{\rm HB}$ is chosen to equal m_0, and then $E = 0$ at this order in lattice-regularized HBChPT.

The contribution of $\mathcal{L}_{\rm MB}^{(2)}$ to the two-point function is purely tree-level and the contribution at the order of $\mathcal{L}_{\rm MB}^{(3)}$ is purely from loop diagrams. The two topologies for loop diagrams are shown in Fig. 2. The diagram with no internal baryon propagator involves the same functions that were used in the previous section for meson masses. For example, the contribution of the charged pion loop to the proton two-point function is

$$\Delta\Gamma_{pp}^{(a)} = \frac{i}{2aF^2}\int_{-\pi/a}^{\pi/a}\frac{{\rm d}^4p}{(2\pi)^4}\left\{x_\pi^2 + \frac{4}{a^2}\sum_\nu\sin^2\left(\frac{ap_\nu}{2}\right)\right\}^{-1}$$
$$\times\left\{\sin(aq_4) - \sin(aq_4 - ap_4) - 2i\sin^2\left(\frac{aq_4}{2}\right) + 2i\sin^2\left(\frac{aq_4 - ap_4}{2}\right)\right\}, \tag{54}$$
$$= -\frac{1}{16a^3F^2}\{\cos(aq_4) - i\sin(aq_4)\}\left\{1 - \frac{1}{2}a^2x_\pi^2W_4(a^2x_\pi^2)\right\}. \tag{55}$$

Because the other diagram in Fig. 2 has an internal baryon propagator, its evaluation is somewhat more involved. The calculation is outlined in Appendix B.

As anticipated by Eq. (53), the final results for the baryon masses are

$$m_B = m_{\rm HB} + \frac{1}{a}\ln(1 + aX_B) \tag{56}$$

where

$$X_B = m_0 - m_{\rm HB} - 2(2x_K^2 + x_\pi^2)b_0 + \gamma_B^{\mathcal{D}}b_{\mathcal{D}} + \gamma_B^{\mathcal{F}}b_{\mathcal{F}} - \frac{1}{3a^3F^2}$$
$$- \frac{1}{16a^3F^2}\sum_{i=\pi,K,\eta}\alpha_B^i\overline{Y}(a^2x_i^2) + \frac{1}{16aF^2}\sum_{i=\pi,K,\eta}x_i^2\beta_B^iW_4(a^2x_i^2). \tag{57}$$

$\overline{Y}(\epsilon^2) \equiv Y_3(\epsilon^2) + Y_4(\epsilon^2)$ is defined by Eq. (A2), and the coefficients α_B^i and β_B^i are given in Table I.

As $a \to 0$ these baryon masses must be identical to the results of dimensional regularization. Unlike dimensional regularization, the results of Eq. (56) contain cubic and linear divergences as $a \to 0$, but these can be absorbed into renormalized parameters as follows,

$$m_0^r = m_0 - \frac{1}{3a^3 F^2} - \frac{(5\mathcal{D}^2 + 9\mathcal{F}^2)}{16a^3 F^2}\overline{Y}(0), \tag{58}$$

$$b_0^r = b_0 + \frac{(13\mathcal{D}^2 + 9\mathcal{F}^2)}{192aF^2}\overline{Y}'(0) - \frac{11}{576aF^2}W_4(0), \tag{59}$$

$$b_{\mathcal{D}}^r = b_{\mathcal{D}} - \frac{3(\mathcal{D}^2 - 3\mathcal{F}^2)}{128aF^2}\overline{Y}'(0) - \frac{5}{384aF^2}W_4(0), \tag{60}$$

$$b_{\mathcal{F}}^r = b_{\mathcal{F}} + \frac{5\mathcal{D}\mathcal{F}}{64aF^2}\overline{Y}'(0), \tag{61}$$

where a prime denotes differentation with respect to the argument. It is convenient to choose $m_{\mathrm{HB}} = m_0^r$. With reference to Appendix A, the $a \to 0$ limit is easily obtained, and is identical to the known dimensional regularization results [11] as required,

$$m_B \to m_0^r - 2(2m_K^2 + m_\pi^2)b_0^r + \gamma_B^{\mathcal{D}}b_{\mathcal{D}}^r + \gamma_B^{\mathcal{F}}b_{\mathcal{F}}^r - \frac{(\alpha_B^\pi m_\pi^3 + \alpha_B^K m_K^3 + \alpha_B^\eta m_\eta^3)}{24\pi F^2}. \tag{62}$$

To conclude this section, consider the pion-nucleon sigma term defined at zero momentum transfer via the Feynman-Hellman theorem,

$$\sigma_{\pi N} = \hat{m}\frac{\partial m_N}{\partial \hat{m}}, \tag{63}$$

where $\hat{m} = (m_u + m_d)/2$. With lattice regularization and exact isospin symmetry, the relation becomes

$$\sigma_{\pi N} = x_\pi^2 \left(\frac{\partial}{\partial(x_\pi^2)} + \frac{1}{2}\frac{\partial}{\partial(x_K^2)} \right) X_N, \tag{64}$$

leading to the following explicit expression,

$$\begin{aligned}
\sigma_{\pi N} = &-2x_\pi^2(2b_0 + b_{\mathcal{D}} + b_{\mathcal{F}}) \\
&+ \frac{3x_\pi^2}{64aF^2}\{W_4(a^2 x_\pi^2) + a^2 x_\pi^2 W_4'(a^2 x_\pi^2) + W_4(a^2 x_K^2) + a^2 x_K^2 W_4'(a^2 x_K^2)\} \\
&+ \frac{5x_\pi^2}{576aF^2}\{W_4(a^2 x_\eta^2) + a^2 x_\eta^2 W_4'(a^2 x_\eta^2)\} \\
&- \frac{9x_\pi^2}{64aF^2}(\mathcal{D} + \mathcal{F})^2\overline{Y}'(a^2 x_\pi^2) \\
&- \frac{x_\pi^2}{64aF^2}(5\mathcal{D}^2 - 6\mathcal{D}\mathcal{F} + 9\mathcal{F}^2)\overline{Y}'(a^2 x_K^2) \\
&- \frac{x_\pi^2}{192aF^2}(\mathcal{D} - 3\mathcal{F})^2\overline{Y}'(a^2 x_\eta^2).
\end{aligned} \tag{65}$$

Using Appendix A, the $a \to 0$ limit is found to be

$$\begin{aligned}
\sigma_{\pi N} \to &-2m_\pi^2(2b_0^r + b_{\mathcal{D}}^r + b_{\mathcal{F}}^r) - \frac{9m_\pi^3}{64\pi F^2}(\mathcal{D} + \mathcal{F})^2 - \frac{m_\pi^2 m_K}{64\pi F^2}(5\mathcal{D}^2 - 6\mathcal{D}\mathcal{F} + 9\mathcal{F}^2) \\
&- \frac{m_\pi^2 m_\eta}{192\pi F^2}(\mathcal{D} - 3\mathcal{F})^2,
\end{aligned} \tag{66}$$

as has been obtained from dimensional regularization [11].

IV. THE BARYON MASSES AT NONZERO LATTICE SPACING

In the previous sections of this work, it has been shown that expressions for the meson masses, the baryon masses and the πN sigma term are the same in both dimensional regularization and lattice regularization in the limit of vanishing lattice spacing. Different expressions are obtained when $a \neq 0$.

Consider first a lattice spacing that satisfies $\pi/a > \Lambda_\chi$. Most lattice QCD simulations are performed with lattice spacings that satisfy this criterion, but with quark masses that are larger than the physical values. If lattice QCD computations are first extrapolated to the continuum, then the chiral extrapolations (i.e. the extrapolations of observables from the simulated quark masses to the physical quark masses) can use the continuum ChPT Lagrangian. Without the initial extrapolation to the continuum, lattice QCD data should obey a lattice ChPT Lagrangian instead of the continuum one. In practice, the $a \neq 0$ effects of lattice-regularized ChPT should be $O(pa/\pi) < O(p/\Lambda_\chi)$, where $p \sim m_\pi$ is a typical momentum. This can now be tested explicitly for the observables under discussion.

For completeness, we also consider a coarser lattice satisfying $\pi/a < \Lambda_\chi$. In this case, Eq. (56) can be expanded in powers of $x_i/(4\pi F)$, x_i/m_0, $(\pi/a)/(4\pi F)$ and $(\pi/a)/m_0$ as follows,

$$
\begin{aligned}
m_B &= m_{\mathrm{HB}} + X_B + \text{ higher order} \\
&= m_B^{(0)} + m_B^{(1)} + m_B^{(2)} + m_B^{(3)} + \text{ higher order},
\end{aligned} \tag{67}
$$

$$
m_B^{(0)} = m_0, \tag{68}
$$

$$
m_B^{(1)} = 0, \tag{69}
$$

$$
m_B^{(2)} = -2(2x_K^2 + x_\pi^2)b_0 + \gamma_B^{\mathcal{D}}b_{\mathcal{D}} + \gamma_B^{\mathcal{F}}b_{\mathcal{F}}, \tag{70}
$$

$$
m_B^{(3)} = -\frac{a}{2}\left(m_B^{(2)}\right)^2 - \frac{1}{3a^3F^2} - \frac{1}{16a^3F^2}\sum_{i=\pi,K,\eta}\alpha_B^i \overline{Y}(a^2 x_i^2)
$$

$$
+\frac{1}{16aF^2}\sum_{i=\pi,K,\eta} x_i^2 \beta_B^i W_4(a^2 x_i^2). \tag{71}
$$

Similar notation will be used for the πN sigma term,

$$
\sigma_{\pi N} = \sigma_{\pi N}^{(0)} + \sigma_{\pi N}^{(1)} + \sigma_{\pi N}^{(2)} + \sigma_{\pi N}^{(3)} + \text{ higher order}, \tag{72}
$$

where

$$
\sigma_{\pi N}^{(0)} = \sigma_{\pi N}^{(1)} = 0, \tag{73}
$$

$$
\sigma_{\pi N}^{(2)} = -2x_\pi^2(2b_0 + b_{\mathcal{D}} + b_{\mathcal{F}}), \tag{74}
$$

and $\sigma_{\pi N}^{(3)}$ is obtained by subtracting $\sigma_{\pi N}^{(2)}$ from Eq. (65). Recall that the parameters b_0, $b_{\mathcal{D}}$ and $b_{\mathcal{F}}$ are not dimensionless; they contain an implicit suppression factor due to their position in $\mathcal{L}_{\mathrm{MB}}^{(2)}$.

The four baryon masses plus the πN sigma term are a set of five observables which depend on five parameters: m_0, b_0, $b_{\mathcal{D}}$, $b_{\mathcal{F}}$ and $\mathcal{D}$. The other axial coupling is obtained from $\mathcal{F} = g_A - \mathcal{D} \approx 1.267 - \mathcal{D}$. To determine discretization errors (i.e. finite-a errors;

differences from continuum results), one could hold the parameters fixed and determine the a-dependence of each observable, or conversely hold the observables fixed and determine the a-dependence of each parameter. In what follows, the experimentally-measured values of the five observables will be used to determine the five parameters at each lattice spacing.

All five observables are linear in m_0, b_0, $b_\mathcal{D}$ and $b_\mathcal{F}$ when the lattice spacing vanishes, but the first term on the right-hand side of Eq. (71) introduces quadratic dependences for nonzero a. This term serves as a reminder that the $a \neq 0$ extension of the continuum HBChPT Lagrangian is not unique. In fact, the term can be eliminated by adding new a-dependent terms to the original (minimal) HBChPT Lagrangian, such as

$$\Delta\mathcal{L}_{\text{MB}}^{(3)} \propto a \text{Tr}\left(\bar{B}_v B_v\right)(\text{Tr}\chi_+)^2 + \dots, \tag{75}$$

with coefficients fixed appropriately. In the present discussion, we will omit the first term on the right-hand side of Eq. (71) from calculations. The particular discretization errors obtained are expected to be representative of a typical lattice ChPT Lagrangian.

Without the first term on the right-hand side of Eq. (71), $\mathcal{D}$ and $\mathcal{F}$ are easily obtained from the Gell-Mann–Okubo relation,

$$\begin{aligned}\Delta_{\text{GMO}} &= \frac{3}{4}m_\Lambda + \frac{1}{4}m_\Sigma - \frac{1}{2}m_N - \frac{1}{2}m_\Xi \\ &= \frac{(\mathcal{D}^2 - 3\mathcal{F}^2)}{64a^3F^2}\left\{4\overline{Y}(a^2x_K^2) - \overline{Y}(a^2x_\pi^2) - 3\overline{Y}(a^2x_\eta^2)\right\}.\end{aligned} \tag{76}$$

With these couplings in hand, $b_\mathcal{D}$ can be extracted from $m_\Sigma - m_\Lambda$, and $b_\mathcal{F}$ from $m_\Xi - m_N$. Finally, b_0 is obtained from $\sigma_{\pi N}$ and m_0 from m_N.

Figure 3 shows the resulting value of each parameter as a function of the lattice cutoff. The "experimental" value of $\sigma_{\pi N}$ was set to 45 MeV [12], and m_η was required to satisfy Eq. (22). As expected, the renormalized parameters are essentially independent of lattice spacing for $\pi/a \gtrsim \Lambda_\chi$; their values in this region are near the dimensional regularized values, which are ultimately attained as $a \to 0$. Significant lattice spacing dependences occur for $\pi/a \lesssim 500$ MeV. The cubic dependence of the unrenormalized parameter m_0 on the inverse lattice spacing is clearly seen.

V. CONCLUSIONS

Lattice regularization is a method for introducing an ultraviolet cutoff directly into the chiral Lagrangian without destroying the Lagrangian's chiral symmetry. As the lattice spacing vanishes, lattice regularization represents an alternative to dimensional regularization. Unlike dimensional regularization, the lattice theory displays power divergences explicitly.

In this work, a lattice ChPT Lagrangian for mesons and baryons has been constructed, and hadron masses and the pion-nucleon sigma term have been calculated to one-loop order.

Researchers have had occasion to apply a nonlattice ultraviolet cutoff to ChPT. (See, for example, Ref. [5].) However, the spacetime lattice is a particularly convenient implementation, due in part to its explicit preservation of chiral symmetry. Another benefit is that the lattice spacing appears directly in the Lagrangian, whereas a nonlattice cutoff would typically be invoked for each Feynman diagram at the time of loop integration.

Lattice regularization is also relevant to lattice QCD simulations, where ChPT is routinely used to extrapolate lattice QCD data as a function of quark masses. The present work demonstrates how discretization errors arising from the difference between lattice ChPT and continuum ChPT can be calculated for a particular lattice ChPT Lagrangian.

ACKNOWLEDGMENTS

[1] S. Weinberg, Physica 96A, 327 (1979); J. Gasser and H. Leutwyler, Ann. Phys. (N.Y.) 158, 142 (1984); J. Gasser and H. Leutwyler, Nucl. Phys. B250, 465 (1985).

[2] G. Colangelo, hep-ph/0001256 (to appear in the 3rd Workshop on Physics and Detectors for DAPHNE), and references therein.

[3] P. J. Ellis and H.-B. Tang, Phys. Rev. C57, 3356 (1998); T. Becher and H. Leutwyler, Eur. Phys. J. C9, 643 (1999).

[4] E. Jenkins and A. V. Manohar, Phys. Lett. B255, 558 (1991); for a review see V. Bernard, N. Kaiser and U.-G. Meissner, Int. J. Mod. Phys. E4, 193 (1995) and U.-G. Meissner hep-ph/9711365 (12th annual HUGS at CEBAF).

[5] J. F. Donoghue and B. R. Holstein, Phys. Lett. B436, 331 (1998); J. F. Donoghue, B. R. Holstein and B. Borasoy, Phys. Rev. D59, 036002 (1999); B. Borasoy, Eur. Phys. J. C8, 121 (1999). See also J. Gasser and H. Leutwyler, Phys. Rep. 87C, 77 (1982), section 10 and appendix C.

[6] See, for example, C. Bernard et. al., Phys. Rev. Lett. 81, 3087 (1998).

[7] S. Myint and C. Rebbi, Nucl. Phys. B 421, 241 (1994); A. R. Levi, V. Lubicz and C. Rebbi, Phys. Rev. D 56, 1101 (1997).

[8] I. A. Shushpanov and A. V. Smilga, Phys. Rev. D59, 054013 (1999).

[9] J. Gasser and H. Leutwyler, Nucl. Phys. B250, 465 (1985).

[10] For example, see H. J. Rothe, *Lattice Gauge Theories, An Introduction*, 2nd edition, World Scientific, 1998.

[11] V. Bernard, N. Kaiser and U.-G. Meißner, Z. Phys. C60, 111 (1993); B. Borasoy and U.-G. Meissner, Phys. Lett. B365, 285 (1996); Ann. Phys. (N.Y.) 254, 192 (1997).

[12] J. Gasser, H. Leutwyler and M. E. Sainio, Phys. Lett. B253, 252 (1991).

APPENDIX A: LIMITS INVOLVING $W_N(\epsilon^2)$ AND $\overline{Y}(\epsilon^2)$

Collected in this appendix are some limits involving the functions, $W_n(\epsilon^2)$ and $\overline{Y}(\epsilon^2) \equiv Y_3(\epsilon^2) + Y_4(\epsilon^2)$, defined by

$$W_n(\epsilon^2) \equiv \int_0^\infty \mathrm{d}x \, I_0^n(x) \exp\left\{-x\left(n + \frac{\epsilon^2}{2}\right)\right\}$$

$$= \int_{-\pi}^{\pi} \frac{\mathrm{d}^n\theta}{(2\pi)^n} \left(n + \frac{\epsilon^2}{2} - \sum_{\mu=1}^{n} \cos\theta_\mu\right)^{-1}, \tag{A1}$$

$$Y_n(\epsilon^2) = 4 \int_0^\infty \mathrm{d}x \, I_0^{n-1}(x) \{I_0(x) - I_0''(x)\} \exp\left\{-x\left(n + \frac{\epsilon^2}{2}\right)\right\}$$

$$= \frac{4}{n} \int_{-\pi}^{\pi} \frac{\mathrm{d}^n\theta}{(2\pi)^n} \left(\sum_{\mu=1}^{n} \sin^2\theta_\mu\right) \left(n + \frac{\epsilon^2}{2} - \sum_{\mu=1}^{n} \cos\theta_\mu\right)^{-1}. \tag{A2}$$

As ϵ vanishes, the functions of interest approach a finite limit,

$$\lim_{\epsilon \to 0} W_3(\epsilon^2) = W_3(0) \approx 0.51, \tag{A3}$$

$$\lim_{\epsilon \to 0} W_4(\epsilon^2) = W_4(0) \approx 0.31, \tag{A4}$$

$$\lim_{\epsilon \to 0} \overline{Y}(\epsilon^2) = \overline{Y}(0) \approx 1.43. \tag{A5}$$

By making use of the asymptotic behaviour of the Bessel function,

$$I_0(x) \overset{x\to\infty}{\to} \frac{\exp(x)}{\sqrt{2\pi x}}, \tag{A6}$$

the following useful limits are obtained,

$$\lim_{\epsilon \to 0} \left\{ \frac{W_3(\epsilon^2) - W_3(0)}{\epsilon} \right\} = -\frac{1}{2\pi}, \tag{A7}$$

$$\lim_{\epsilon \to 0} \left\{ \frac{W_4(\epsilon^2) - W_4(0)}{\epsilon} \right\} = 0, \tag{A8}$$

$$\lim_{\epsilon \to 0} \left\{ \frac{\overline{Y}(\epsilon^2) - \overline{Y}(0)}{\epsilon} \right\} = 0. \tag{A9}$$

When comparing lattice regularized results to dimensional regularization, the following relation is helpful,

$$\lim_{\epsilon \to 0} \left\{ \frac{W_4(\epsilon^2) - W_4(0)}{\epsilon^2} \right\} = \lim_{\epsilon \to 0} \left\{ \frac{\ln \epsilon}{4\pi^2} \right\} + \text{ constant.} \tag{A10}$$

To understand this connection to the logarithm, integrate Eq. (A6) to produce the exponential integral,

$$Ei(-x) = - \int_1^\infty \mathrm{d}t \, \frac{\exp(-xt)}{t}, \tag{A11}$$

and then notice that

$$\lim_{x \to 0} \left(\frac{Ei(-x)}{\ln(x)} \right) = 1. \tag{A12}$$

14

Finally, the calculation of the πN sigma term makes use of the following limits,

$$\lim_{\epsilon \to 0} \left\{ \epsilon W_3'(\epsilon^2) \right\} = -\frac{1}{4\pi}, \tag{A13}$$

$$\lim_{\epsilon \to 0} \left\{ \epsilon W_4'(\epsilon^2) \right\} = 0, \tag{A14}$$

$$\lim_{\epsilon \to 0} \left\{ \epsilon \overline{Y}'(\epsilon^2) \right\} = 0, \tag{A15}$$

and the identity

$$Y_n'(\epsilon^2) = \frac{2}{n} - \left(2 + \frac{\epsilon^2}{n} \right) W_n(\epsilon^2). \tag{A16}$$

APPENDIX B: A LOOP CALCULATION

This appendix outlines the calculation of the Feynman diagram in Fig. 2 which contains an intermediate baryon propagator. For definiteness, the contribution of a charged-pion loop to the proton is chosen.

The diagram represents the following integral,

$$\Delta\Gamma_{pp}^{(b)} = -ia \lim_{\epsilon \to 0} \int_{-\pi/a}^{\pi/a} \frac{\mathrm{d}^4 p}{(2\pi)^4} \left\{ x_\pi^2 + \frac{4}{a^2} \sum_\nu \sin^2 \left(\frac{ap_\nu}{2} \right) \right\}^{-1}$$
$$\times \left\{ \sin(aq_4 + ap_4 + i\epsilon) + 2i \sin^2 \left(\frac{aq_4 + ap_4 + i\epsilon}{2} \right) \right\}^{-1}$$
$$\times \left\{ \frac{i\sqrt{2}}{aF} (\mathcal{D} + \mathcal{F}) \sum_\mu S_\mu \sin(ap_\mu) \right\}^2. \tag{B1}$$

The precise limits of integration deserve some thought. One might consider integrating from $-\min(\pi/a, \pi/a + q_\mu)$ through $\min(\pi/a, \pi/a - q_\mu)$ since this would ensure that both the meson and nucleon momenta remain within the first Brillouin zone. However, choosing $v = (0, 0, 0, 1)$ and working in the proton's rest frame makes q_μ suppressed by the inverse baryon mass, so the limits of Eq. (B1) are accurate to the order we are working. These choices also lead to $S_4 = 0$.

Notice that an "$i\epsilon$" term has been included in the nucleon denominator of Eq. (B1), so that the singularity can be treated correctly. Using

$$\sin(aq_4 + i\epsilon) + 2i \sin^2 \left(\frac{aq_4 + i\epsilon}{2} \right) = e^{-\epsilon} \{ \sin(aq_4) + i[e^\epsilon - \cos(aq_4)] \}, \tag{B2}$$

and a property of the Pauli-Lubanski vector,

$$2S_\mu S_\nu = \frac{1}{2} (v_\mu v_\nu - \delta_{\mu\nu}) + [S_\mu, S_\nu], \tag{B3}$$

one arrives at the following form,

$$\Delta\Gamma_{pp}^{(b)} = \lim_{\epsilon \to 0} \left(\frac{-(\mathcal{D} + \mathcal{F})^2}{4aF^2} \right) \int_{-\pi/a}^{\pi/a} \frac{\mathrm{d}^4 p}{(2\pi)^4} \left\{ x_\pi^2 + \frac{4}{a^2} \sum_\nu \sin^2 \left(\frac{ap_\nu}{2} \right) \right\}^{-1}$$

$$\times \sum_{k=1}^{3} \sin^2(ap_k) \left\{ 1 + \left(\frac{\sinh \epsilon}{\cosh \epsilon - \cos(ap_4)} \right) \right\}. \tag{B4}$$

The piece without $\sinh \epsilon$ is expressible in terms of $Y_4(a^2 x_\pi^2)$, and the piece containing $\sinh \epsilon$ can be expressed in terms of $Y_3(a^2 x_\pi^2)$. The functions $Y_n(\epsilon^2)$ are discussed in Appendix A. The final result is

$$\Delta\Gamma_{pp}^{(b)} = -\frac{3}{32a^3 F^2} (\mathcal{D} + \mathcal{F})^2 \left\{ Y_3(a^2 x_\pi^2) + Y_4(a^2 x_\pi^2) \right\}. \tag{B5}$$

TABLE I. Coefficients that appear in the baryon masses.

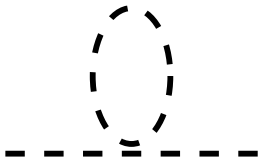|	$B = N$	$B = \Sigma$	$B = \Xi$	$B = \Lambda$
α_B^π	$(9/4)(\mathcal{D} + \mathcal{F})^2$	$\mathcal{D}^2 + 6\mathcal{F}^2$	$(9/4)(\mathcal{D} - \mathcal{F})^2$	$3\mathcal{D}^2$
α_B^K	$(1/2)(5\mathcal{D}^2 - 6\mathcal{D}\mathcal{F} + 9\mathcal{F}^2)$	$3(\mathcal{D}^2 + \mathcal{F}^2)$	$(1/2)(5\mathcal{D}^2 + 6\mathcal{D}\mathcal{F} + 9\mathcal{F}^2)$	$\mathcal{D}^2 + 9\mathcal{F}^2$
α_B^η	$(1/4)(\mathcal{D} - 3\mathcal{F})^2$	$\mathcal{D}^2$	$(1/4)(\mathcal{D} + 3\mathcal{F})^2$	$\mathcal{D}^2$
β_B^π	$3/4$	$3/2$	$3/4$	$1/2$
β_B^K	$3/2$	1	$3/2$	$5/3$
β_B^η	$5/12$	$1/6$	$5/12$	$1/2$
$\gamma_B^\mathcal{D}$	$-4x_K^2$	$-4x_\pi^2$	$-4x_K^2$	$-4x_\eta^2$
$\gamma_B^\mathcal{F}$	$4(x_K^2 - x_\pi^2)$	0	$-4(x_K^2 - x_\pi^2)$	0

FIG. 1. The only meson loop topology which contributes to a meson mass at one-loop order in ChPT.

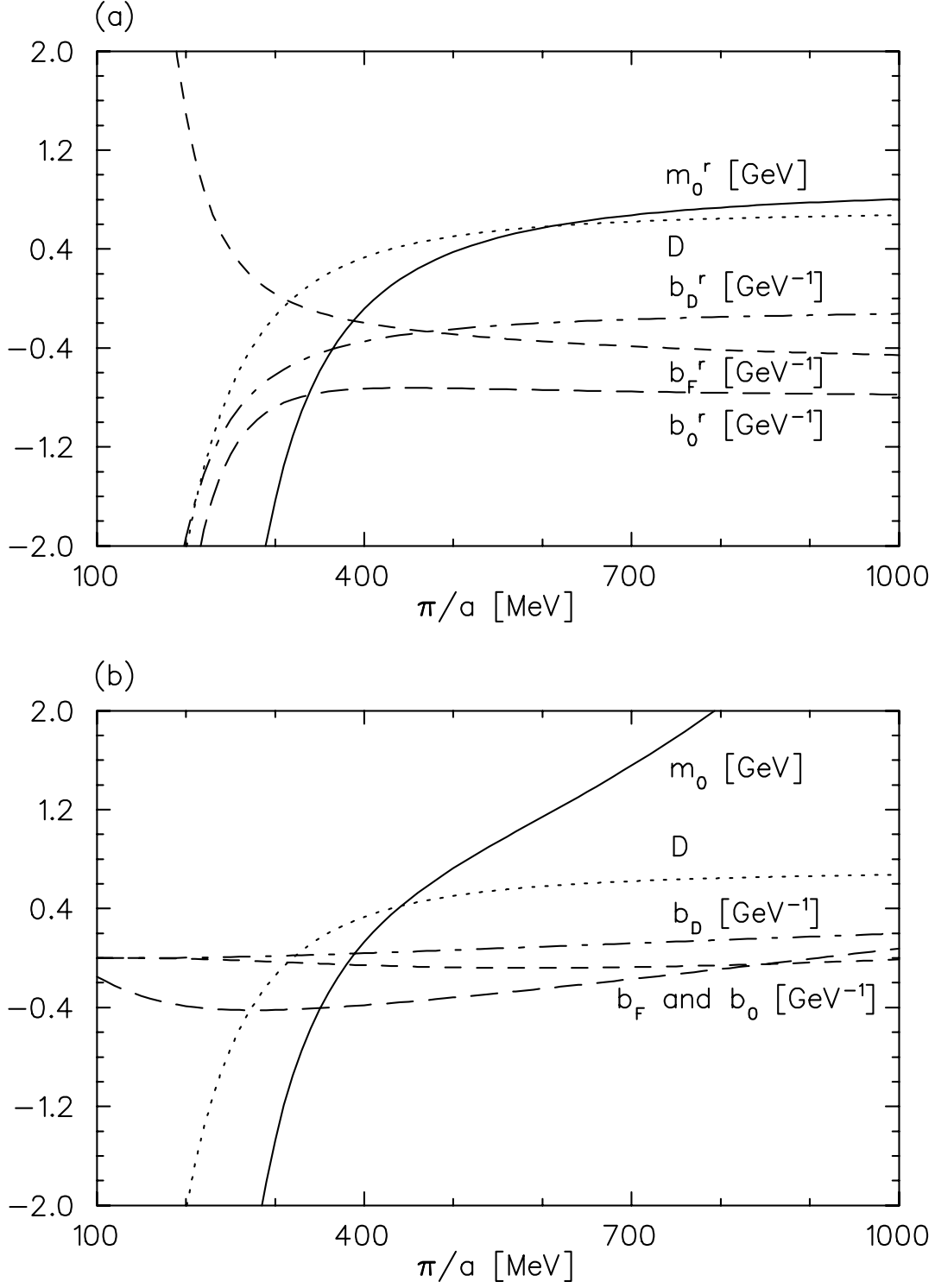FIG. 2. The two loop topologies which contribute to a baryon mass at leading-loop order in HBChPT.

FIG. 3. Five parameters, obtained by fitting to the experimental values of g_A, $\sigma_{\pi N}$ and the four masses of the octet baryons. The sixth parameter is easily obtained as $\mathcal{F} = g_A - \mathcal{D}$. The fit to experimental values is redone for each lattice cutoff, π/a. Both the (a) renormalized and (b) unrenormalized values of the parameters are plotted.